Chromosome Motion during Attachment to the Vertebrate Spindle: Initial Saltatory-like Behavior of Chromosomes and Quantitative Analysis of Force Production by Nascent Kinetochore Fibers

Stephen P. Alexander* and Conly L. Rieder*‡

*Wadsworth Center for Laboratories and Research, Empire State Plaza, Albany, New York 12201-0509, and ‡School of Public Health, State University of New York, Albany, New York 12201

Abstract. Before forming a monopolar attachment to the closest spindle pole, chromosomes attaching in newt (*Taricha granulosa*) pneumocytes generally reside in an optically clear region of cytoplasm that is largely devoid of cytoskeletal components, organelles, and other chromosomes. We have previously demonstrated that chromosome attachment in these cells occurs when an astral microtubule contacts one of the kinetochores (Hayden, J., S. S. Bowser, and C. L. Rieder. 1990. *J. Cell Biol.* 111:1039–1045), and that once this association is established the chromosome can be transported poleward along the surface of the microtubule (Rieder, C. L., and S. P. Alexander. 1990. *J. Cell Biol.* 110:81–95). In the study reported here we used video enhanced differential interference contrast light microscopy and digital image processing to compare, at high spatial and temporal resolution (0.1 μm and 0.93 s, respectively), the microtubule-mediated poleward movement of attaching chromosomes and poleward moving particles on the spindle. The results of this analysis demonstrate obvious similarities between minus end-directed particle motion on the newt pneumocyte spindle and the motion of attaching chromosomes. This is consistent with the hypothesis that both are driven by a similar force-generating mechanism. We then used the Brownian displacements of particles in the vicinity of attaching chromosomes to calculate the apparent viscosity of cytoplasm through which the chromosomes were moving. From these data, and that from our kinetic analyses and previous work, we calculate the force-producing potential of nascent kinetochore fibers in newt pneumocytes to be ~0.1–7.4 $\times$ 10^{-6} dyn/microtubule. This is essentially equivalent to that calculated by Nicklas (Nicklas, R. B. 1988. *Annu. Rev. Biophys. Biophys. Chem.* 17:431–449) for prometaphase (4 $\times$ 10^{-6} dyn/microtubule) and anaphase (5 $\times$ 10^{-6} dyn/microtubule) chromosomes in *Melanoplus*. Thus, within the limits of experimental error, there appears to be a remarkable consistency in force production per microtubule throughout the various stages of mitosis and between groups of diverse taxonomic affinities.

THE equal distribution of replicated genetic material is dependent on the highly coordinated movement of chromosomes. Past observations clearly reveal that this movement arises from the formation of a birefringent fiber (i.e., a kinetochore fiber [K-fiber][1]), composed primarily of microtubules (MTs), which firmly connects the kinetochore to the polar region (reviewed in references 38, 39, 46). The exact role that kinetochore MTs (K-MTs) play in chromosome movement is, however, controversial. For example, it is unclear whether K-MTs directly generate and/or transmit the mitotic forces, whether they act simply as "tracks" along which kinetochores move, or whether they act as an extrinsic governor to regulate chromosome velocity generated by a mechanistically separate force generator (5, 6, 19, 25, 46).

Previous work has focused on chromosome motion during anaphase, when the K-fiber is fully formed and chromosome movement is slow, synchronous, and predictable in its direction and duration, and its velocity may be governed (25). Indeed, novel technological and methodological approaches have recently been used to obtain important information concerning MT dynamics, force production, and kinetochore function in metaphase and anaphase cells (9, 18, 19, 24, 26). In summary these studies reveal that the spindle can produce much more force than is actually required to move the chromosome at the speeds seen during anaphase, and that the kinetochore plays a more active role in force production than previously envisioned. In contrast to metaphase and anaphase, little data is available regarding kinetochore function and force production during prometaphase when bipolar attached chromosomes congress to the metaphase plate (20, 25). Moreover, no such data are available for attaching chromosomes, when the K-fiber is forming and putative velocity governors are absent or in the early stages of activation. This

1. *Abbreviations used in this paper*: K-fiber, kinetochore fiber; K-MT, kinetochore microtubule; MT, microtubule; NEB, nuclear envelope breakdown; NP, newt pneumocyte; r.m.s., root mean square.

lack of information arises, in part, from the sudden and unpredictable nature of K-fiber formation, which occurs immediately after nuclear envelope breakdown (NEB) in a region of the cell crowded with chromosomes (see reference 50). In this respect newt pneumocytes (NPs) possess a number of unique advantages for examining the initial stages of K-fiber formation and spindle transport at a high resolution light microscopic level (reviewed in references 39, 42). These cells remain extremely flat throughout mitosis, and the spindle forms in an optically clear area of cytoplasm largely devoid of cytoskeletal components and organelles (15). As a result both the centrosomes (i.e., spindle poles) and the primary constrictions on the chromosomes are clearly visible. Furthermore, chromosomes that are separated from the spindle poles by >30 μm are delayed in attaching to the spindle (41). When these chromosomes finally attach, they do so within the clear area of cytoplasm at the periphery of the aster where MT density is extremely low. The process of attachment and the subsequent behavior of chromosomes can therefore be examined in unsurpassed detail within the living cell by correlative microscopic methods.

Using the NP system Hayden et al. (10) observed that chromosome attachment is mediated by a single astral microtubule which interacts with one of the kinetochores. Moreover, once this connection is established the chromosome can be transported poleward along the surface of the microtubule 25 times faster than anaphase chromosomes (41), by a mechanism that does not depend on MT depolymerization. To further characterize this process we used high temporal and spatial resolution methods to compare the detailed behavior of attaching chromosomes with that of saltating particles within the same NPs. We than augmented this analysis with measurements of apparent viscosity in the region of attaching chromosomes. The results of our study provide new insight into the behavior of chromosomes prior to and during K-fiber formation, and allow us to estimate the force producing potential of nascent K-fibers.

Materials and Methods

Primary lung cell cultures from the newt *Taricha granulosa* were grown in Rose chambers (42) and observed with a Nikon Microphot microscope as detailed by Rieder and Alexander (41). DIC optics were used with a 40× objective (NA = 0.85) to maintain the kinetochore and pole in the video field. Simultaneous focus on the pole and kinetochore was essential for precise plotting of the chromosome-to-pole distance. Total irradiation (546 nm) was reduced by shuttering the quartz halogen or tungsten light source with a Uniblitz shutter controlled by an XT-class computer. Analogue signals from a Dage MTI 70 Newvicon video camera were sent to a Hamamatsu DVS 3000 digital image processor for digital enhancement.

Fixed noise and shading arising in the optical system was eliminated by background subtraction, and input images were averaged in real time (two to eight frames). Image enhancement through grey-scale transformation was performed in real time and the processed images were recorded with a Panasonic TQ 2025 optical memory disk recorder (OMDR), controlled by an XT-class computer using Laser Base II software (SMI systems, Ft. Lauderdale, FL). Framing rates were selected from 0.93 to 4.1 s and synchronized with the shutter operation so that the illumination commenced and halted at a predetermined interval before (0.25 s), and after (0.1 s), a frame was recorded by the OMDR.

Spindle Viscosity Measurements

To determine apparent spindle viscosities we recorded Brownian displacements of natural cytoplasmic inclusions within the clear zone of cells used for chromosome motion analysis. These particles were always selected in a region lacking other organelles and were located in the vicinity of chromosomes delayed in attaching. Such areas are known to be largely devoid of MTs, actin and keratin (15, 41), and therefore the possibilities of non-Brownian motion were largely eliminated. To confirm that all movements were Brownian we plotted the measured mean-square displacements of each particle against time. In such a plot pure diffusion will produce a straight line, whereas diffusion superimposed with directed motion or caged (restricted) diffusion will produce positive and negative curves, respectively (52).

The principles and limitations of viscosity determination using Brownian motion are described by Taylor (page 176 in reference 55). We differed only in the use of the Einstein-Stokes equation:

$$\eta = \frac{kTt}{3\pi a\bar{X}^2} \quad (1)$$

(where η = viscosity in poise; k = Boltzman constant; T = absolute temperature; t = time interval in s; a = particle radius; $\bar{X}$ = particle displacement per time interval t), which does not require the use of grid lines to measure displacement. The potential error introduced by wall effects was minimized by selecting only those particles located in the clear zone remote from other optically detectable inclusions. 50 displacements for 3 particles in each of 10 cells were measured, and the results substituted in Eq. 1 for calculation of apparent spindle viscosities.

Viscosity measurements were standardized by recording the Brownian motion of polybead-hydroxylate monodisperse microspheres (Polysciences, Inc., Warrington, PA) in glycerol solutions under the same optical and recording conditions as the chromosome sequences. Microspheres of 1.04 (SD = 0.006) and 0.47 μm (SD = 0.006) diameter were recorded in 50, 80, 95, and 100% aqueous solutions of glycerol. 90 frames were analyzed for each of the glycerol concentrations. To establish whether stage drift or slide/coverslip movements were significant, we plotted the mean square displacement with time for 100-nm gold particles attached to a coverslip and mounted in glycerol.

Chromosome Stretching

To measure the extent of chromosome stretching we compared chromosome length before attachment with that during steady-state motion into the aster. Accurate length measurements were determined, using calibrated cursors, along the central groove between the daughter chromatids, or when this groove was not clear, along a line that longitudinally bisects the chromosome arms. Chromosomes which became entangled in their own arms were not included in the analysis. A total of 9 chromosomes of the 15 analyzed were usable for length change measurements.

Data Analysis

To facilitate accurate location and high-resolution tracking of the primary constriction or particles, images were expanded electronically two to eight times (two to four times for chromosomes and four to eight times for particles) during image reprocessing. Using the Hamamatsu's distance measuring system, one cursor was superimposed on the kinetochore or edge of the primary constriction, and another on the clearly visible spindle pole. The pixel coordinates for both, and the distance separating them for each frame analyzed, were entered manually into a Lotus (Lotus Development Corporation, Cambridge, MA) spreadsheet. The cursors had previously been calibrated under the same optical conditions as the recordings, using the 0.62-μm frustule spacing of the diatom *Pleurasigma angulatum*. Total geometrical distortion in our system (introduced by combined effects of the optical system, video camera and digitizer; 13) was calculated at ~4.8% between two perpendicular planes located in the central video field. Since geometrical decalibration was not performed, we minimized this error by routinely calibrating cursors in the plane of the chromosome movement by rotating the *Pleurasigma* preparation. Difficulty was experienced in the precise sizing of particles tracked for Brownian motion in the clear zone. We found that all microsphere standards observed in glycerol or water were inflated in the primary and reprocessed digitized images, and that this inflation increased with the level of contrast enhancement even when measured in a plane perpendicular to the plane of DIC separation. As the slope of the intensity transformation function is increased (60) the apparent particle size is increased. Apparent inflation can range from 1.45× with 1.05-μm spheres to 2.3× with 0.51-μm spheres. These inflations are most likely a combination DIC optical effects, camera "blooming" (13), and grey scale

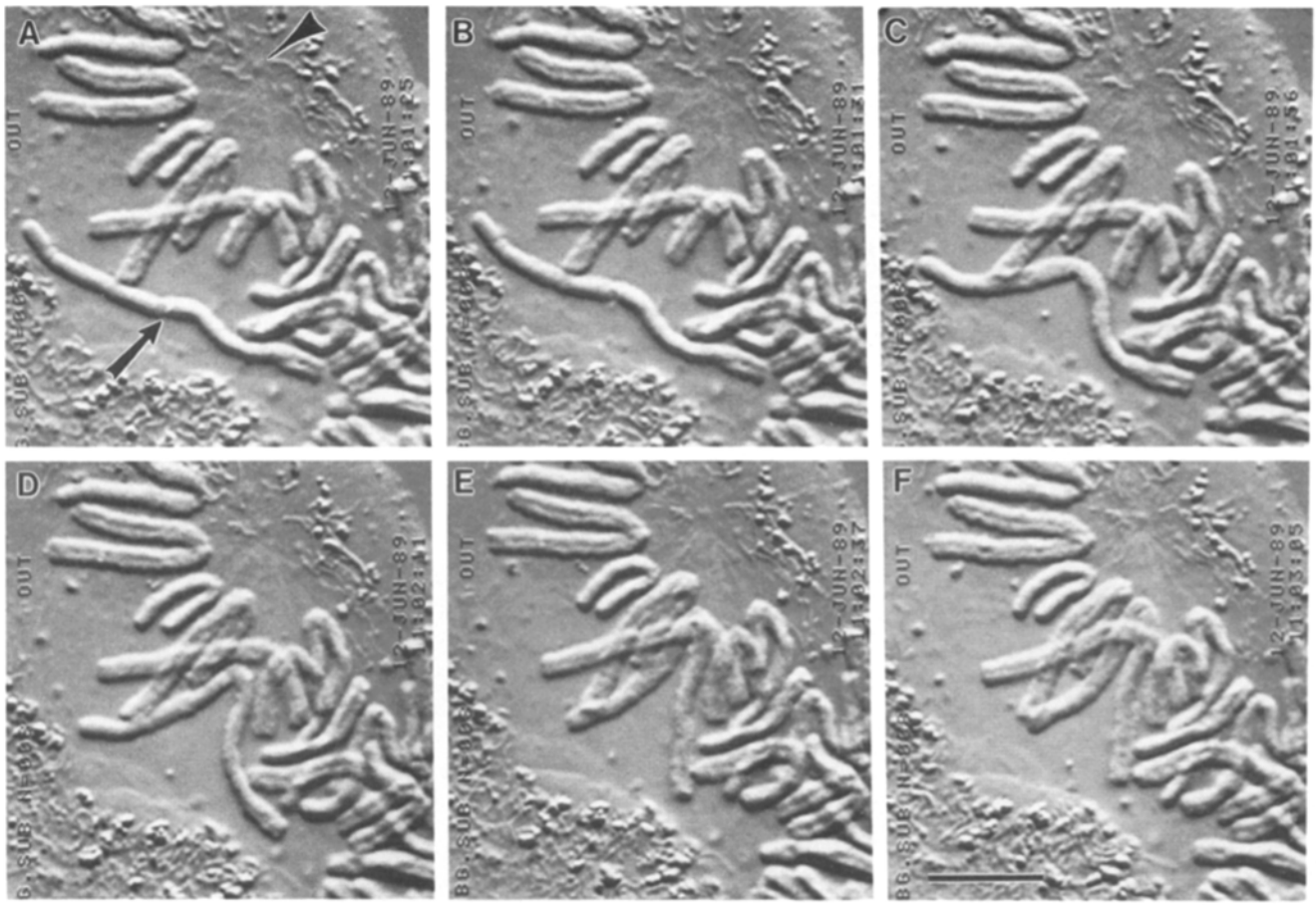

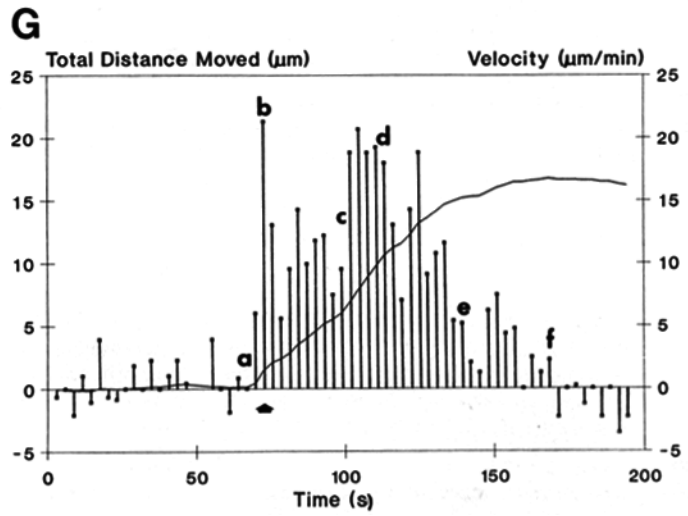

Figure 1. (*A–F*) Selected DIC videomicrographs, from a time-lapse recording, of a chromosome (*arrow* in *A*) attaching to the spindle and moving toward the pole (*arrowhead* in *A*). Time (h:min:s) is visible in upper right-hand side of each micrograph. The chromosome, located in a distinct clear area of cytoplasm, attaches in *B*, and moves poleward with variable velocity until reaching a stable position in *F*. In *G* the instantaneous chromosome velocities (*bars*) and total distance moved (cumulative; *line*) are plotted. The letters within the plot correspond to micrographs *A–F*. Bar, 10 μm.

losses during digitization. To circumvent these problems we recorded 1.05-, 0.51-, 0.4-μm-diam microspheres in a glycerol solution of ~300 cP for use as standards for cursor calibration. These calibrations were used only for measuring the diameters of similarity sized particles within the clear zone and were not used for linear distance measurements.

To test the accuracy of locating the center of particles, we ran two-dimensional intensity distribution profiles on particles in random frames of analyzed sequences, and compared the computed centroid with that determined manually by the analyst. For the tracking of Brownian motion, both cursors were initially superimposed at the center of the particle, the recording advanced one or more frames, and one cursor re-centered on the same particle in the succeeding frame. Displacement in the x- and y-axis, and total displacement in one framing interval were then manually transferred to a Lotus spreadsheet.

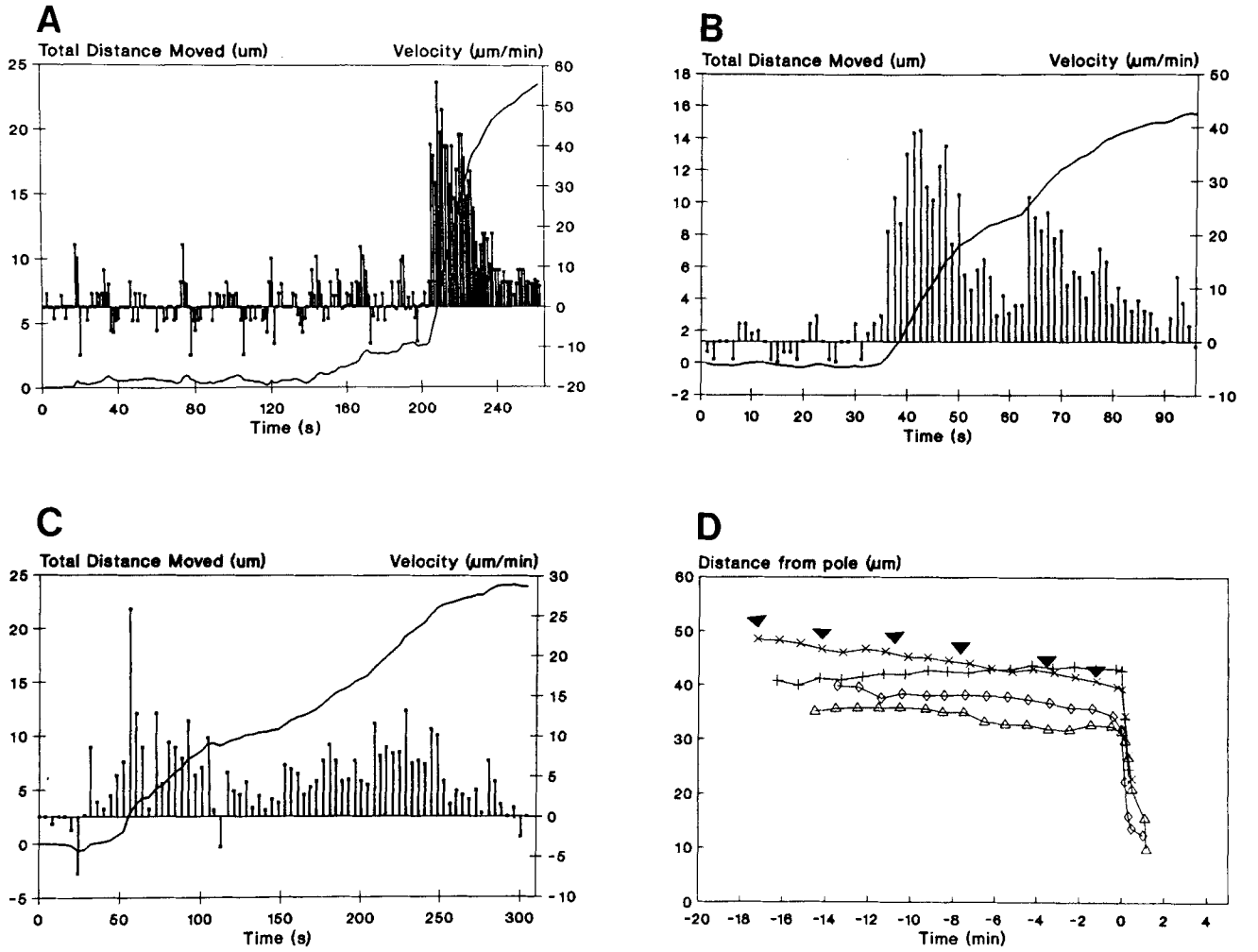

Figure 2. (*A–C*) Three plots showing instantaneous velocities (*bars*) and cumulative distance moved (*line*) for chromosomes delayed in attachment. Note the extended connection phase in *A* with strong tugs; the weaker but more typical tugs during the connection phase in *B*, and in *C*, the sudden stop followed by a brief negative velocity, i.e., directed away from the pole. In *D* the distance from the spindle pole vs. time is plotted for four chromosomes delayed in attachment. For each of the plots time zero was taken as the point of attachment and initiation of the transit phase (see text). The plot marked with arrowheads is from a chromosome which drifted from a position ~49 μm distal to the closest pole to ~41 μm, at which point it attached and accelerated poleward.

Results

A Kinetic Analysis of Chromosome Monoorientation

The distinct area of clear cytoplasm in which NP chromosomes are located following NEB (see Fig. 1) enables precise frame-by-frame tracking of chromosomes and particles on the same spindle. The following kinetic analysis of monoorientation is based on the behavior of 15 chromosomes, all of which were delayed (20 to >200 min) by natural events in attaching to the NP spindle (see reference 41). Four of these chromosomes were chemically fixed during poleward movement and were therefore used only for the analysis of initial attachment. For this study we have arbitrarily divided the process of attachment into the following four phases: preconnection, connection, transit, and pole associated. The details of kinetochore and chromosome behavior during each of these phases are described below.

Changes in the chromosome-to-pole distance are the sum of chromosome motion and astral movements. However, on a frame-by-frame basis astral movements are small when compared with Brownian displacements of the kinetochore region, and consequently their contribution to changes in the chromosome-to-pole distance is largely insignificant. Prometaphase cells in which the aster was seen to move significantly during chromosome attachment were excluded from this analysis. Therefore, changes in the chromosome-to-pole distance with time can be plotted as an accurate measure of chromosome velocity.

Preconnection Phase. For any chromosome, the duration between NEB and the initiation of rapid non-Brownian kinetochore displacements is extremely variable and depends on the chromosome-to-pole distance at the time of NEB. In those cases where a chromosome is situated <25–30 μm from a pole, the preconnection phase will be extremely short lived. Indeed, since this applies to the great majority of chromosomes in NPs (and other cells, see references 45, 50), most if not all chromosomes attach to the forming spindle within 2 min of NEB (15). By contrast, chromosomes located >30 μm from the closest pole, or those which are sterically hindered by other chromosomes, may remain in the pre-connection phase for up to 5 h. During

this time the chromosome-to-pole distance may remain constant (0–70 s; Fig. 1) or be gradually reduced by Brownian motion, cytoplasmic flow, and/or aster migration (140–200 s; Fig. 2 *A*). Although this movement is gradual and velocities are low (<3 μm/min), the resultant reduction in chromosome-to-pole distance increases the probability of attachment. Chromosomes located >50 μm from the pole may never attach to the spindle unless they subsequently achieve a closer position. The preconnection "drift" of four chromosomes is illustrated in Fig. 2 *D*. The plot noted by arrowheads in this figure is that of a chromosome that drifted from a position ~49-μm distal to the closest pole to ~41 μm, at which point it attached and accelerated poleward. In some cases the drift of a chromosome actually increases its distance from the pole, but unless this drift takes the chromosome out of the 50 μm astral "casting range" the chromosome will eventually attach and move rapidly towards a pole (e.g., see plot marked with crosses in Fig. 2 *D*). With this type of plot the point of chromosome attachment appears as an acute angle in the slope of the distance vs. time plot, but at higher temporal resolution it is apparent that attachment may be preceded by a series of poleward tugs.

Connection Phase. This phase is characterized by one or more tugs toward the pole and/or shoves away from the pole (Fig. 2, *A* and *B*). These tugs, which are brief (3–10 s) result in little or no net decrease in the chromosome-to-pole distance and exhibit velocities ranging from ±5 to ±15.5 μm/min. Plots of distance vs. time produce a horizontal line (0–140 s in Fig. 2 *a*; 0–35 s in Fig. 2 *B*), or an extremely gradual slope (140–200 s in Fig. 2 *A*), which is easily distinguished from the main poleward movement. A poleward tug is often followed immediately by movement away from the pole with a velocity of similar, or smaller, magnitude. In long connection phases (>100 s), such as that illustrated in Fig. 2 *A*, the chromosome-to-pole distance may be gradually reduced as a result of an exaggerated imbalance between tugs and shoves (140–200 s in Fig. 2 *A*). The typical duration of a connection phase was exceedingly variable, ranging from less than our most rapid framing rate (0.93 s) to >200 s with a mean of 46.7 ± 17.6 s (n = 11). The ±5 to ±15.5 μm/min transient positive and negative velocities seen during the connection phase far exceeded the velocities shown by anaphase chromosomes in these cells (~2.3 μm/min; 42). However, connection-phase velocities are three to four times slower than those seen during the transit phase.

Transit Phase. The initiation of this phase is characterized by a rapid poleward acceleration of the kinetochore to velocities of ≥15 μm/min (*arrowhead* in Fig. 1 *G*). In comparison to the connection phase the kinetochore exhibits a more continuous poleward movement, i.e., stops and reversals are infrequent.

The velocities exhibited by the kinetochore during the transit phase are extremely variable with common fluctuations of ±10 to ±20 μm/min in periods of 1–5 s. Peak instantaneous velocities averaged 33.7 ± 3.6 μm/min (n = 11) with a maximum of 55.7 μm/min and mean velocities were 12.6 ± 1.4 μm/min (n = 11). The initiation of the transit phase is reflected, on the cumulative distance curve, by an acute angle as the chromosome-to-pole distance is rapidly decreased. However, this traditional method of presenting chromosome motion data masks the fine-scale temporal fluctuations that are apparent when instantaneous velocities are plotted on a frame-by-frame basis. Kinetochore acceleration at the onset of the transit phase averaged 406 μm/min², (n = 14) with a maximum of 1,640 μm/min² (calculated over a single framing interval).

Although the poleward accelerations exhibited by kinetochores during the initial stages of the transit phase are rapid, the chromosomes do not necessarily achieve maximum velocity during this time. On average 31% (±7.5%) of the total time passes before chromosomes reach their maximum recorded velocities, and only 3 of 11 chromosomes followed to the end of the transit phase achieved maximum, or near maximum, velocities in the latter half. In one case the chromosome reached its maximum velocity in the latter part of the transit phase after rapid negative velocities and a period of virtually no net movement.

Irrespective of the velocity at which it was previously moving poleward, a chromosome could abruptly halt, and immediately show a brief negative velocity, at any point in the transit phase (Fig. 2 *C*). 4 of 11 chromosomes exhibited this behavior; on one occasion we observed a chromosome halt without reversal.

Pole Associated. At the completion of the transit phase the chromosome is associated with a single pole. The average distance that a monooriented chromosome adopts at the end of the transit phase, relative to the astral center, is highly variable. In bipolar spindles the chromosome may approach within 1 μm of the pole (see reference 2; 43). By contrast, in monopolar or anaphase-like prometaphase spindles the chromosomes characteristically maintain an average position 10–15 μm from the astral center (reviewed in references 39, 42). In all cases, however, monooriented chromosomes that are associated with a spindle pole exhibit the oscillatory (sequential positive and negative velocities) behavior previously described by Bajer (2).

Chromosome Stretching

The amount of chromosome stretching during steady state motion into the aster varied from 0.3 to 15.7% with a mean of 5.6% (±1.8%, n = 9). No correlation was demonstrated between chromosome length prior to attachment, and the extent of stretch (r = −0.0096, $P < 0.05$).

Particle Saltations

Our data on particle motion are summarized in Table I and four examples of the velocity profiles are shown in Fig. 3. Particles selected for this analysis were located in the clear area distal to the monooriented chromosomes, or in close proximity to late-attaching chromosomes. In three cases the particle paths correspond to a ray drawn from the centrosome through the primary constriction of an attaching chromosome, and the remaining particles were all moving along rays pointed toward a pole.

To temporally separate individual saltations an arbitrary quiescent period of ≥15 s was designated to mark the end of a single saltation. Furthermore, a theoretical lower velocity threshold for saltatory motion was defined, below which all movements were regarded as attributable to Brownian motion. This arbitrary threshold can be calculated using Rebhun's (36) method for determining the root mean square (r.m.s.) Brownian displacement of a known diameter particle in a medium of specified viscosity. For a 0.4-μm-diam parti-

Table I. Characteristics of Poleward Particle Transport in the Vicinity of Late-attaching Chromosomes

Particle	Excursion	Excursion period	Distance moved	Maximum velocity
		s	*μm*	*μm/min*
1	a	4.2	4.2	79.6
	b	4.2	2.4	53.1
2		7.3	6.4	84.8
3		3.7	5.0	97.3
4		9.9	9.0	102.1
5		6.2	4.0	50.4
6		6.2	4.4	49.2
7	a	3.7	1.9	41.4
	b	10.0	7.6	79.9
	c	2.5	3.0	80.4
8	a	1.2	1.6	76.9
	b	1.2	1.9	90.9
	c	5.0	7.2	110.7
Mean		5.0 ± 0.8	4.5 ± 0.7	76.7 ± 6.1

Particles in the clear area (see text) and in the near vicinity of late-attaching chromosomes were tracked on a frame-by-frame basis during pole-directed movement. An arbitrary quiescent period of ⩾15 s was designated to separate individual poleward movements consisting of one or several excursions. The time period of each excursion, total distance moved, and maximum velocity attained during the excursion are all recorded.

cle in cytoplasm of 282 cP (see below), at our largest and smallest framing intervals, we calculate velocities of 3.0–5.4 μm/min respectively. Since r.m.s. = the standard deviation (36), four times this value (22 μm/min) provides a conservative criterion for separating saltatory movements from Brownian motion. Using this criterion we found that the characteristics of particle motion into the aster are: (*a*) rapid accelerations; (*b*) short excursions (mean = 5.02 s; n = 13) with high velocities during which particles travel on average 4.5 μm (n = 13), and (*e*) rapid decelerations that are often followed by brief velocity reversals. During the main excursions, instantaneous velocities are rarely constant and can fluctuate by 20–60 μm/min. It is notable that the highest recorded particle velocity of 110 μm/min is almost two times the maximum recorded chromosome velocity in these cells, and the mean path length of excursions (4.5 μm) is approximately one-third that of typical monoorienting chromosome path lengths (14.5 μm).

Viscosity Calculations

The error (13–35%) involved in calculating the viscosity of known glycerol standards from the Brownian movement of microspheres was very similar to that noted by Taylor (55).

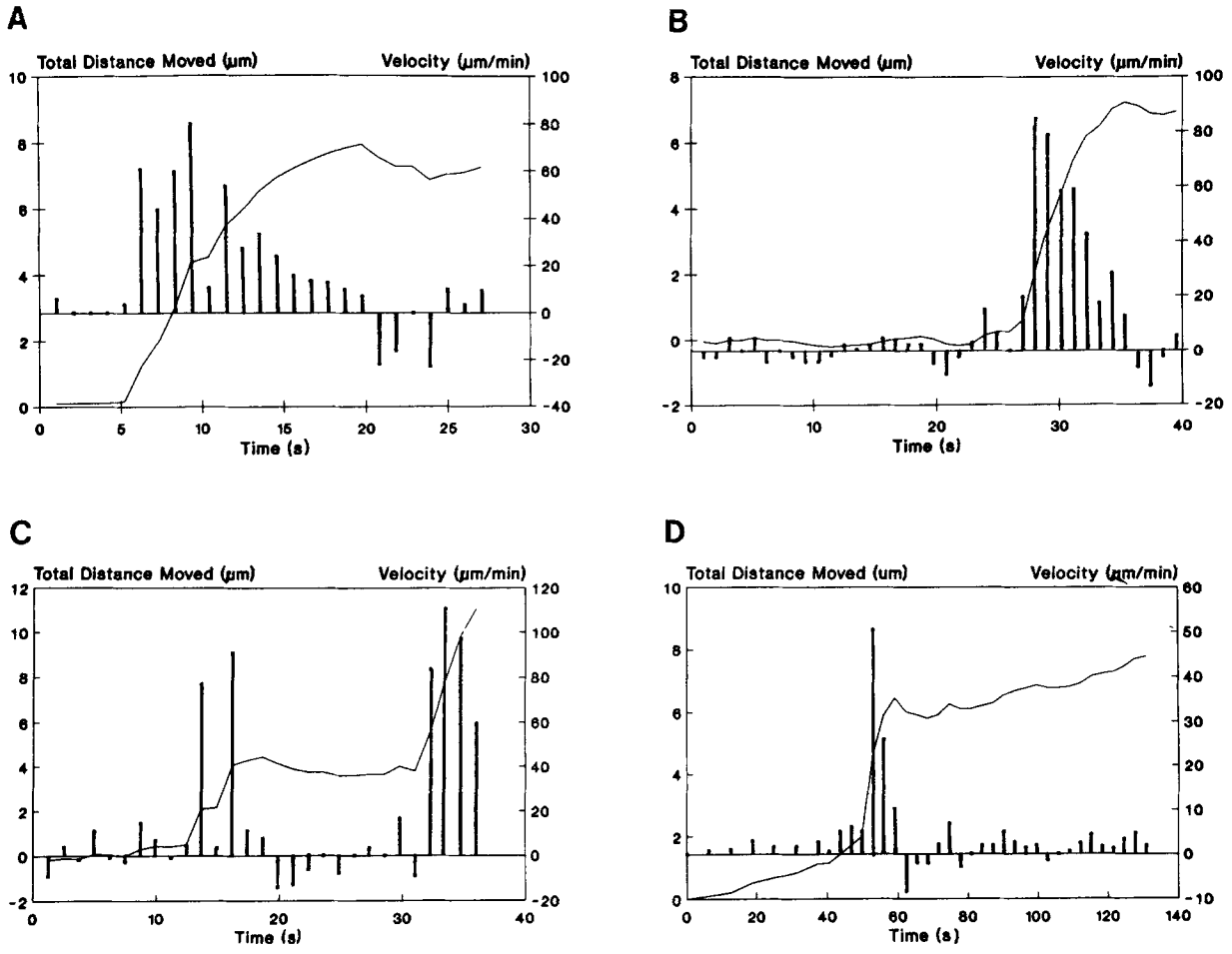

Figure 3. (*A–D*) Four examples of particle saltations on the NP spindle. Bars represent instantaneous velocities and the thin line is a plot of total distance moved (cumulative) vs. time. The particles were all located in the clear area close to chromosomes delayed in attachment, and were saltating along paths corresponding to rays drawn from the centrosome.

Table II. Apparent Viscosities Calculated from Brownian Displacements of Particles Located in the Immediate Vicinity of Attaching Chromosomes

Cell	Particle	Apparent viscosity	Mean apparent viscosity
		cP	*cP*
1	A	89	
	B	57	86
	C	112	
2	A	105	
	B	199	289
	C	562	
3	A	305	
	B	444	388
	C	415	
4	A	115	
	B	93	104
5	A	470	470
6	A	107	
	B	772	439
7	A	141	
	B	132	199
	C	324	
Mean			282 cP

Apparent cytoplasmic viscosity was calculated from the Brownian displacements of particles in the clear area (see text) using the Einstein-Stokes equation. All particles were confirmed by mean-square displacement vs. time plots, to be diffusing freely.

Plots of the mean-square displacement vs. time interval produced a straight line relation indicating that the observed motion represented diffusion (52) and that the margin of error was not due to superimposed velocities or restriction of diffusion. Actual measurements made within the clear area of NPs, near the chromosomes analyzed in this study, revealed apparent viscosities ranging from 57 to 772 cP (Table II), with a mean of 282 cP. This range of viscosities agrees closely with Taylor's (55) values for the cytoplasm surrounding the spindle in newt fibroblasts. 90% of the particles chosen for analysis were confirmed, by linear relationships in the mean-square displacement plots, to be diffusing freely; all those showing a nonlinear relationship were excluded from viscosity calculations. We found no significant correlation between particle size and viscosity ($R = 0.2$, $P < 0.05$).

Discussion

On the basis of previous findings in NPs (10, 41) we have hypothesized that the molecular motors responsible for early prometaphase chromosome motion are located within the corona on the surface of the kinetochore, and that these motors interact with the surface of astral MTs to attach the chromosome to the spindle and move it towards the minus MT end. Since the velocity at which a monoorienting chromosome moves poleward in response to K-fiber formation (37, 41, 45, 56) approaches that displayed in vitro by cytoplasmic dynein (8, 27, 28), it has been proposed (41) that the poleward movement of monoorienting (and anaphase; 59) chromosomes is mediated by cytoplasmic dynein bound to the kinetochore. This latter hypothesis has gained considerable support from the recent indirect immunofluorescent demonstrations that the centromere region of prophase and prometaphase chromosomes contain cytoplasmic dynein (30, 53).

If the molecular motors responsible for the poleward movement of organelles and attaching chromosomes along the surface of astral MTs are the same, then the behavior of translocating particles and attaching chromosomes would be expected to possess a number of common characteristics.

Chromosome Behavior during K-Fiber Formation

The salient features of chromosome motion after a monopolar attachment are rapid initial acceleration, high but extremely variable poleward velocities, and infrequent stops with or without reversals. Based on the classic definition of saltatory transport (34, 36), the motion of attaching NP chromosomes could be regarded as saltatory. The presence of a quiescent period followed by virtually instantaneous acceleration and rapid linear excursions, occasional pauses, and a return to a period of relative quiescence, are all traits shared by attaching chromosomes and saltating particles. However, the motion of attaching NP chromosomes differs from Rebhun's definition of saltatory motion in that the velocity during one translocation is not constant, the end of a poleward movement (transit) is rarely marked with a stop that is as abrupt as the start, and the number of pauses/reversals is low.

When examined in the context of more recent studies on particle transport, which used methods enabling much greater temporal resolution ($\leq$1 s), the differences between the poleward motion of particles and attaching chromosomes appear minor. Indeed, the extreme variability in instantaneous velocities exhibited by attaching chromosomes are features of particle/organelle saltations in a variety of living cells (1, 3, 61), and in vitro systems (7), and constant velocities may last only for periods of 0.1–2 s. The significance of these velocity fluctuations is presently unclear, although Weiss et al. (61) attributed them to Brownian events owing to the absence of a common frequency component. Whether or not this motion can be attributed to Brownian events can be tested by calculating the velocity of a particle that would result from Brownian motion alone. We did this using Rebhun's (36) method which estimates the r.m.s. displacement due to Brownian motion. A value of 0.05 μm was obtained (particle of 0.4 μm diam; viscosity of 50 cP), which corresponds to a velocity of only 30 μm/min. Since this value is far below the velocity variations of 120 μm/min observed by Weiss et al. (61), Brownian motion cannot account for the observed velocity variations. A similar evaluation of the centromere region reveals that Brownian motion would produce velocities of $\sim$2.8 μm/min and, since tethered chromosomes will show restricted Brownian motion, this is likely to be an underestimate. We therefore conclude that the observed velocity variations seen during poleward chromosome movement are not a manifestation of Brownian motion superimposed on active transport. Since inertia can be largely ignored (22, 25, 33), and assuming the movement is load-limited, chromosome velocity is determined by the total force generated divided by the frictional resistance of the chromosome (25), as in Eq. 2:

$$V = F/\eta S \qquad (2)$$

(where S = a factor that accounts for the size and shape of a chromosome, η = cytoplasmic viscosity in poise). In this case, the fluctuations in NP chromosome instantaneous velocities must be attributed to either a change in applied force or variations in drag acting on the chromosome as it moves poleward. With load-limited chromosome movement, large variations in apparent cytoplasmic viscosity would result in fluctuations of chromosome velocity. Alternatively if the V_{max} of the motor acts as an intrinsic governor, then our calculations could only apply to the lower limit of force production, i.e., the minimum required to move the chromosome at a given velocity. In this case viscosity variations would be unlikely to affect chromosome velocities. The presence of only a single MT during connection, and the large size of newt chromosomes, make it likely that initial chromosome movement during the connection and early transit phases may be load limited. Indeed, the concept of load-limited chromosome motion fits well with the observations. For example, the gradual slowing of chromosomes which are nearing a pole at the end of a saltation may be caused by additional load such as increased viscosity (densely packed MTs?), centripetal polar ejection forces (43; reviewed in reference 46) or the incorporation of an extrinsic velocity governor (4, 12, 23, 25). The drag associated with small saltating particles driven by the same motor would, theoretically, be insufficient to limit velocity, and therefore particles would be expected to travel much faster than chromosomes. Furthermore, their small surface area would minimize the effect of polar ejection forces, resulting in a rapid stop when the motor switches off instead of slowing gradually in response to opposing forces. This is exactly what we have observed: small particles traveling poleward at twice the rate of chromosome movement, with sudden stops. It is highly probable that the V_{max} of the motor itself limits the maximum velocity of small particles on the spindle.

The final difference we noted between the movement of attaching NP chromosomes and typical saltations (34–36) is the apparent sparsity of pauses exhibited by chromosomes. However, particles on the same spindle as attaching chromosomes show similar numbers of pauses (<3) during a poleward movement and very brief reversals rarely reaching 10% of poleward velocities. Using the "vector scalar ratio" (3) as a measure of net progress in one direction, we find that chromosomes and particles on the same spindle have similar high ratios of 0.96 ± 0.016 and 0.98 ± 0.02, respectively, values that correspond closely to those of saltations in spinal cord, chick dorsal root ganglion, and brain cells (3). This strong tendency to move in one direction with few pauses and reversals results in a more continuous motion than that defined by Rebhun (36) as saltatory transport. Such motion prompted Weiss et al. (61) to propose a new classification of active motion and, using this classification, we categorize NP chromosome and particle motion on the spindle, as "Interrupted I," where the prominent fluctuations in velocity result in stops but only rarely in reversals.

Cytoplasmic dynein fulfills many of the criteria for a retrograde translocator (27, 28, 49, 51). This fact together with the recent immuno-localization of dynein at kinetochores and along spindle fibers (30, 53), strongly support the contention that dynein is the common force-generating mechanism for pole-directed chromosome motion (58). Our data are consistent with this hypothesis since there are obvious similarities between the characteristics of MT-mediated poleward movement of attaching chromosomes and that of particles on the NP spindle. Attaching prometaphase NP chromosomes move along the surface of MTs (41) at velocities approaching those of particles on the spindle, exhibit great variations in velocity, and may show stops and starts during movement to the pole.

Chromosome Behavior Before K-Fiber Formation

Poleward tugs are often observed at the primary constriction prior to the main poleward transit (21, 45; this study). To determine whether these motions are attributable to Brownian forces we calculated the r.m.s. path of a theoretical particle under similar conditions (see above). To be conservative we assumed that only the primary constriction region is displaced during a tug, and that this is equivalent to a 2-μm-diam sphere. Using our average viscosity of 282 cP we find an r.m.s. displacement which exceeds the standard deviation of path lengths that would be expected for Brownian motion, by a factor of 7×. Therefore, it is clear that Brownian motion does not account for the tugs observed in the connection phase.

The active nature of these observed tugs suggests a poleward force acting at the kinetochore. In light of previous results (10, 30, 41, 53) we conclude that the poleward tugs seen at the kinetochore during the preconnection phase are produced by kinetochore corona-bound cytoplasmic dynein interacting with an astral MT. The resultant poleward force developed from this interaction is enough to displace the kinetochore region and often a large part of the chromosome, but the attachment (between the corona and the kinetochore plate, the dynein and the corona, and/or the dynein and the MT) may be sufficiently weak to break under the full load of viscous drag imparted by the chromosome. The recoil behavior observed after tugs and stops during poleward chromosome movement may be explained by chromosome elasticity. Typical early prometaphase NP chromosomes can be stretched up to 16% of their length during unhindered poleward movement. As a result, any loss of attachment will likely be manifested by a rapid but brief recoil of the kinetochore region.

Force Production by Forming K-Fibers

The force required to move a chromosome can be calculated using the equation:

$$F = \eta S V \tag{3}$$

(where η is the cytoplasmic viscosity, S is a factor which accounts for the size and shape of the chromosome, and V is the chromosome velocity; 22). From our study we accurately know the maximum velocity at which a given chromosome moves poleward during K-fiber formation. To calculate S we used Eqs. 3 and 4 from Nicklas (22) for a prolate ellipsoid moving with its long axis parallel and perpendicular to the direction of movement respectively (29). Since chromosomes rarely attach with their arms parallel to the direction of subsequent movement, but do form a characteristic "V" shape as they move poleward, we used an average value for S calculated from Eqs. 3 and 4 (22). The apparent viscosity of the cytoplasm through which the chromosome

Table III. Comparison of Force Required to Move Chromosomes

Method of calculation	Organism	Stage	Kinetochore fiber	Calculated force	
				Total	Per MT
				dyn × 10⁻⁶	
(a) Maximum observed values	*T. granulosa*	Prometaphase	Nascent	7.4	–
(b) Mean observed values	*T. granulosa*	Prometaphase	Nascent	1.2	–
(c) From example in Fig. 2 *a*	*T. granulosa*	Prometaphase	Nascent	2.3	–
(d) From Rieder and Alexander (1990), Fig. 6	*T. granulosa*	Prometaphase	Single MT	1.3	1.3
(e) From Rieder and Alexander (1990), Fig. 11	*T. granulosa*	Prometaphase	Single MT	0.8	0.8
(f) Nicklas, 1983: micromanipulation	*M. differentialis*	Prometaphase	Fully formed	30	4
(g) Nicklas, 1983: micromanipulation	*M. sanguinipes*	Anaphase	Fully formed	70	5

is moving can be calculated from the Brownian displacements of adjacent particles (55). This method provides only an approximate apparent viscosity since several factors, including wall effects (55) and the non-Newtonian properties of cytoplasm (31, 32), contribute unavoidable error. However, by limiting our measurements to the clear area surrounding the forming spindle we have minimized wall effects resulting from the interaction of particles with cytoskeletal elements and other particles. Moreover, since the particles that we analyzed for Brownian displacements showed velocities from 1.5 to 5.1 μm/min, the shear gradient range was within the same order of magnitude as attaching chromosomes (55). As a result, we are able to largely ignore errors introduced by the non-Newtonian properties of cytoplasm.

Our calculated mean viscosity value within the region of attaching chromosomes in prometaphase *Taricha granulosa* NPs is 282 cP. This value is consistent with those calculated by Taylor (55) for fibroblasts from the newt *Triturus viridens* (260, 350, and 240 cP for prophase, metaphase, and anaphase, respectively). Using similar methods Schaap and Forer (48) calculated the apparent viscosity of anaphase I crane fly spermatocyte cytoplasm to be 40–120 cP in the temperature range 20–25°C. However, neither these workers nor Taylor (55) were able to confine their measurements to an optically clear cytoplasmic region devoid of cytoskeletal elements. More recent calculations of apparent viscosities in many types of interphase cells, using various methodologies (see reference 57 for references), produced values ranging from 20 (Swiss 3T3 cells; 16) to 10^8 cP (squid axoplasm; 47). Moreover, there appears to be some relation between the size of the particles used for analysis and the apparent viscosity (47). This is most probably due to networks of cross-linked proteins and filaments, that impart viscoelastic and thixotropic qualities to the cytoplasm (44, 54), and produce an effective mesh size above which the apparent viscosity is dramatically increased (14). The lack of any large-order cytoplasmic network detectable by thick/thin section EM in NPs (15) suggests that our calculated apparent viscosities are a close approximation to that experienced by chromosomes during poleward transit.

From Table III (*c*) it can be seen that a force of 2.3×10^{-6} dyn is required to move a chromosome poleward at 56 μm/min, and that a single MT can produce a force of 1.3×10^{-6} dyn (Table III, *d*). These forces are only 30–50 times less than the maximum force measured directly by microneedle deflections during anaphase in grasshopper (*Melanoplus*) spermatocytes (Table III, *g*) (24). Furthermore it is apparent that force per MT during anaphase in *Melanoplus* is only three to four times that generated per MT in NPs during poleward movement at 26.6 μm/min (Table III, *d*). More significantly, since NP chromosomes can accelerate to >50 μm/min immediately after attachment, and since this movement is likely produced by the interaction of a single MT with the kinetochore (41), the force generated per MT in prometaphase NPs is remarkably similar to that measured by Nicklas (24) for grasshopper spermatocytes in anaphase. In addition force per MT values from prometaphase NPs are within a factor of 10 of those for prometaphase and anaphase grasshopper spermatocytes (24). Thus, within the limits of experimental error, there appears to be a remarkable consistency in force production per MT not only between groups of diverse taxonomic affinities, but also throughout the various stages of mitosis. Because of this finding we feel justified in comparing our results from prometaphase NPs with those obtained by Nicklas (24, 25) for prometaphase and anaphase grasshopper spermatocytes.

An important consideration at this point is the relationship between the number of MTs impinging on the kinetochore and the total force generated. Our recent model (41) proposes that force generation is not strictly dependent on the number of MTs present at the kinetochore since it assumes that the force-generating sites within the corona could be equally dispersed along several or numerous MTs. If this were the case, one would expect that the maximum prometaphase forces produced by a fully formed K-fiber would not be significantly greater than those produced by a few MTs interacting with the kinetochore. Force production per MT appears to range from 0.8 to 7.4×10^{-6} dyn which, as noted above, is close to that measured in *Melanoplus* (4×10^{-6} dyn). The values for *Melanoplus* were calculated by dividing the maximum measured force generated by a mature K-fiber, by the number of K-MTs impinging on the kinetochore (24). Since we know the approximate force per MT in NPs, we would predict a total force in the range $1.6–15 \times 10^{-5}$ dyn for a mature K-fiber (20 MTs/K-fiber × 0.8 to 7.4×10^{-6} dyn) assuming that total force is proportional to the number of MTs (11). Although this range is consistent with the findings of Nicklas (24) it is not possible at present to determine

how the force is distributed among MTs terminating at the kinetochore and exactly how many MTs are required to reach maximum force producing potential. If there were a finite limit as to how far corona material could extend along a MT and simultaneously transmit force to the chromosome, force per MT may initially be high and then decrease as more MTs enter the KC and the force-producing sites are redistributed (40). Further addition of MTs will only increase total force production until all the force-producing molecules are attached, after which total force should remain constant. Clearly the question of proportionality between total force produced and the number of MTs at the kinetochore requires more data. Our analysis suggest that the margin of excess force potential, calculated to be 10,000× for *Melanoplus* anaphase chromosomes (24), may not be available to attaching NP chromosomes. Nicklas's calculation of the force required to move chromosomes was based on small chromosomes moving slowly through an assumed maximum viscosity of 100 cP (from 55). However, Taylor's data shows that a more accurate maximum apparent viscosity would be in the range 1,000–1,350 cP with averages of 260, 350, and 240 cP for prophase, metaphase, and anaphase, respectively. Using our maximum apparent viscosity of 772 cP, measured in the vicinity of large rapidly moving chromosomes, we find that a force of 7.4×10^{-6} dyn is required for movement. Since we have established that force per-MT is very similar in *Melanoplus* and NPs, there is some value in comparing our maximum force requirement (7.4×10^{-6} dyn) with the maximum prometaphase force measured in *Melanoplus* (8×10^{-5} dyn; 25). If our comparison is valid then the margin of excess force potential available to attaching newt chromosomes may be closer to 10× rather than the 10,000× available for *Melanoplus* anaphase chromosomes. Therefore differences in the reserve force-producing potential appear to be a reflection of varying conditions, such as chromosome size, velocity, and cytoplasmic viscosity, rather than variations in the characteristics of the motor itself. Such would be the case if the molecular motors responsible for chromosome motion in *Taricha* and *Melanoplus* share the same origin and have been conserved throughout evolution.

The authors express their appreciation to Drs. S. S. Bowser, J. H. Hayden, C. A. Mannella, E. D. Salmon, and R. B. Nicklas for invaluable discussions on many aspects of the work presented in this manuscript, and two anonymous reviewers whose comments vastly improved the final form. We also thank Mr. A. J. DeMarco and Mr. R. Cole for excellent technical help throughout the long evolution of this project, and Ms. Carolyn Wieland for administrative assistance.

The work was supported in part by National Institutes of Health GMS grant RO1-40198 (to C. L. Rieder) and Biotechnological Resource Grant RR 01219 awarded by the Division of Research Resources, Department of Health and Human Resources/Public Health Service to support the Wadsworth Center's Biological Microscopy and Image Reconstruction Resource as a National Biotechnological Resource.

Received for publication 28 September 1990 and in revised form 28 January 1991.

Note Added in Proof. Recently Wordeman et al. (Wordeman, L., E. R. Steuer, M. P. Sheetz, and T. Mitchison. 1991. Chemical subdomains within the kinetochore domain of isolated CHO mitotic chromosomes. *J. Cell Biol.* In press) have convincingly localized dynein in the fibrous corona on the distal face of the kinetochore plate, using immunogold electron microscopy.

References

1. Allen, R. D., J. Metuzals, I. Tasaki, S. Brady, and S. P. Gilbert. 1982. Fast axonal transport in squid giant axon. *Science (Wash. DC).* 218: 1127–1129.
2. Bajer, A. S. 1982. Functional autonomy of monopolar spindle and evidence for oscillatory movement in mitosis. *J. Cell Biol.* 93:33–48.
3. Breuer, A. C., C. N. Christian, M. Henkart, and P. G. Nelson. 1975. Computer analysis of organelle translocation in primary neuronal cultures and continuous cell lines. *J. Cell Biol.* 65:562–576.
4. Forer, A. 1974. Possible roles of microtubules and actin-like filaments during cell division. *In* Cell Cycle Controls. G. M. Padilla, I. L. Cameron, and A. M. Zimmerman, editors. Academic Press, Inc., New York. 319–336.
5. Forer, A. 1988. Do anaphase chromosomes chew their way to the pole or are they pulled by actin? *J. Cell Sci.* 91:449–453.
6. Fuge, H. 1989. Rapid kinetochore movements in *Mesostoma ehrenbergii* spermatocytes: action of antagonistic chromosome fibers. *Cell Motil. Cytoskel.* 13:212–220.
7. Gelles, J., B. J. Schnapp, and M. P. Sheetz. 1988. Tracking kinesin-driven movements with nanometer-scale precision. *Nature (Lond.).* 331:450–453.
8. Gibbons, I. R. 1988. Dynein ATPases as microtubule motors. *J. Biol. Chem.* 263:15837–15840.
9. Gorbsky, G. J., P. J. Sammak, and G. G. Borisy. 1987. Chromosomes move poleward in anaphase along stationary microtubules that coordinately disassemble from their kinetochore ends. *J. Cell Biol.* 104:9–18.
10. Hayden, J., S. S. Bowser, and C. L. Rieder. 1990. Kinetochores capture astral microtubules during chromosome attachment to the mitotic spindle: direct visualization in live newt lung cells. *J. Cell Biol.* 111:1039–1045.
11. Hays, T. S., and E. D. Salmon. 1990. Poleward force at the kinetochore in metaphase depends on the number of kinetochore microtubules. *J. Cell Biol.* 110:391–404.
12. Hyman, A. A., and T. J. Mitchison. 1990. Modulation of microtubule stability by kinetochores in vitro. *J. Cell Biol.* 110:1607–1616.
13. Inoué, S. 1987. Video microscopy. Plenum Publishing Corp., New York/London.
14. Luby-Phelps, K., D. L. Taylor, and F. Lanni. 1986. Probing the structure of cytoplasm. *J. Cell Biol.* 102:2015–2022.
15. Mandeville, E. C., and C. L. Rieder. 1990. Keratin filaments restrict organelle migration into the forming spindle of newt pneumocytes. *Cell Motil. and Cytoskeleton.* 15:111–120.
16. Mastro, A. M., and Kieth, A. D. 1984. Diffusion in the aqueous compartment. *J. Cell Biol.* 99:180s–187s.
17. McIntosh, J. R., and Koonce, M. P. 1989. Mitosis. *Science (Wash. DC).* 246:622–628.
18. Mitchison, T. J. 1989. Polewards microtubule flux in the mitotic spindle: evidence from photoactivation of fluorescence. *J. Cell Biol.* 109:637–652.
19. Mitchison, T., L. Evans, E. Schulze, and M. Kirschner. 1986. Sites of microtubule assembly and disassembly in the mitotic spindle. *Cell.* 45:515–527.
20. Mitchison, T. J. 1989. Chromosome alignment at mitotic metaphase: balanced forces or smart kinetochores? *In* Cell Movement. Kinesin, Dynein, and Microtubule Dynamics. Vol. 2. Alan R. Liss, Inc., New York. 421–430.
21. Mole-Bajer, J., A. Bajer, and A. Owczarzak. 1975. Chromosome movements in prometaphase and aster transport in the newt. *Cytobios.* 13:45–65.
22. Nicklas, R. B. 1965. Chromosome velocity during mitosis as a function of chromosome size and position. *J. Cell Biol.* 25:119–135.
23. Nicklas, R. B. 1975. Chromosome movement: current models and experiments on living cells. *In* Molecular and Cell Movement. S. Inoue and R. E. Stephens, editors. Raven Press, Ltd., New York. 97–117.
24. Nicklas, R. B. 1983. Measurements of the force produced by the mitotic spindle in anaphase. *J. Cell Biol.* 97:542–548.
25. Nicklas, R. B. 1988. The forces that move chromosomes in mitosis. *Annu. Rev. Biophys. Biophys. Chem.* 17:431–449.
26. Nicklas, R. B. 1989. The motor for poleward chromosome movement in anaphase is in or near the kinetochore. *J. Cell Biol.* 109:2245–2255.
27. Paschal, B. M., and R. B. Vallee. 1987. Retrograde transport by the microtubule-associated protein map 1C. *Nature (Lond.).* 330:181–183.
28. Paschal, B. M., H. S. Shpetner, and R. B. Vallee. 1987. Map 1C is a microtubule activated ATPase which translocates microtubules in vitro and has dynein-like properties. *J. Cell Biol.* 105:1273–1282.
29. Perrin, F. 1934. Mouvement Brownien d'un ellipsoide (I). Dispersion diélectrique pour des molécules ellipsoidales. *J. Phys. et radium.* 5:ser 1:497.
30. Pfarr, C. M., M. Cove, P. M. Grissom, T. S. Hays, M. E. Porter, and J. R. McIntosh. 1990. Cytoplasmic dynein is localized to kinetochores during mitosis. *Nature (Lond.).* 345:263–265.
31. Pollard, T. D. 1984. Molecular architecture of the cytoplasmic matrix. *In* White Cell Mechanisms: Basic Science and Clinical Aspects. Alan R. Liss, Inc., New York. 75–86.

32. Porter, K. R. 1984. The cytomatrix: a short history of its study. *J. Cell Biol.* 99:3s–12s.
33. Purcell, E. M. 1977. Life at low Reynolds number. *Am. J. Physics.* 45: 3–11.
34. Rebhun, L. I. 1959. Studies of early cleavage in the surf clam, *Spisula solidissima*, using methylene blue and toluidine blue as vital stains. *Biol. Bull.* 117:518–545.
35. Rebhun, L. I. 1963. Saltatory particle movements and their relation to the mitotic apparatus. *In* The Cell in Mitosis. L. Levine, editor. Academic Press, Inc., New York. 67–103.
36. Rebhun, L. I. 1972. Polarized intracellular particle transport: saltatory movements and cytoplasmic streaming. *Int. Rev. Cytol.* 32:93–131.
37. Rickards, G. K. 1975. Prophase chromosome movements in living house cricket spermatocytes and their relationship to prometaphase, anaphase and granule movements. *Chromosoma (Berl.).* 49:407–455.
38. Rieder, C. L. 1982. The formation, structure and composition of the mammalian kinetochore and kinetochore fiber. *Int. Rev. Cytol.* 79:1–58.
39. Rieder, C. L. 1990. Formation of the astral mitotic spindle: ultrastructural basis for the centrosome:kinetochore interaction. *Electron Microsc. Rev.* 3:269–300.
40. Rieder, C. L. 1991. Mitosis: towards a molecular understanding of chromosome behavior. *Curr. Opin. Cell Biol.* 3:59–66.
41. Rieder, C. L., and S. P. Alexander. 1990. Kinetochores are transported poleward along a single astral microtubule during chromosome attachment to the spindle in newt lung cells. *J. Cell Biol.* 110:81–96.
42. Rieder, C. L., and R. Hard. 1990. Newt lung epithelial cells: cultivation, use and advantages for biochemical research. *Int. Rev. Cytol.* 122:153–220.
43. Rieder, C. L., E. A. Davison, L. C. W. Jensen, L. Cassimeris, and E. D. Salmon. 1986. Oscillatory movements of monooriented chromosomes and their position relative to the spindle pole results from the ejection properties of the aster and half-spindle. *J. Cell Biol.* 103:581–591.
44. Ris, H. 1985. The cytoplasmic filament system in critical point-dried whole mounts and plastic-embedded sections. *J. Cell Biol.* 100:1474–1487.
45. Roos, U.-P. 1976. Light and electron microscopy of rat kangaroo cells in mitosis. III. Patterns of chromosome behavior during pro-metaphase. *Chromosoma (Berl.).* 54:363–385.
46. Salmon, E. D. 1989. Microtubule dynamics and chromosome movement. *In* Mitosis: Molecules and Mechanisms. J. H. Hyams and B. R. Brinkley, editors. Academic Press, Inc., New York. 118–181.
47. Sato, M., T. Z. Wong, and R. D. Allen. 1984. Rheological properties of living cytoplasm: endoplasm of *Physarum* plasmodium. *J. Cell Biol.* 97:1089–1097.
48. Schaap, C. J., and A. Forer. 1979. Temperature effects on anaphase chromosome movement in the spermatocytes of two species of crane flies (*Nephrotoma saturalis loew* and *Nephrotoma ferruginea fabricus*). *J. Cell Sci.* 39:29–52.
49. Schnapp, B. J., and T. S. Reese. 1989. Dynein is the motor for retrograde axonal transport of organelles. *Proc. Natl. Acad. Sci. USA.* 86:1548–1552.
50. Schrader, F. 1953. The Movements of Chromosomes in Cell Division. Columbia University Press, New York. 170 pp.
51. Schroer, T. A., E. R. Seuer, and M. P. Sheetz. 1989. Cytoplasmic dynein is a minus end-directed motor for membranous organelles. *Cell.* 56: 937–946.
52. Sheetz, M. P., S. Turney, H. Qian, and E. L. Elson. 1989. Nanometer-level analyses demonstrate that lipid flow does not drive membrane glycoprotein movements. *Nature (Lond.).* 340:284–288.
53. Steuer, E. R., L. Wordeman, T. A. Schroer, and M. P. Sheetz. 1990. Localization of cytoplasmic dynein to mitotic spindles and kinetochores. *Nature (Lond.).* 345:266–268.
54. Stossel, T. P. 1982. The structure of cortical cytoplasm. *Philos. Trans. R. Soc. Lond. B Biol. Sci.* 299:275–289.
55. Taylor, E. W. 1965. Brownian and saltatory movements of cytoplasmic granules and the movement of anaphase chromosomes. *In Proc. 4th Int. Cong. Rheology. Part 4. Symp. Biorheology.* A. L. Copley, editor. Interscience, New York. 175–191.
56. Tippit, D. H., J. D. Pickett-Heaps, and R. Leslie. 1980. Cell division in two large pennate diatoms *Hantzschia* and *Nitzschia*. III. A new proposal for kinetochore function during prometaphase. *J. Cell Biol.* 86:402–416.
57. Valberg, P. A., and D. F. Albertini. 1985. Cytoplasmic motions, rheology, and structure probed by a novel magnetic particle method. *J. Cell Biol.* 101:130–140.
58. Vallee, R. 1990. Dynein and the kinetochore. *Nature (Lond.).* 345:206–207.
59. Vallee, R. B., H. S. Shpetner, and B. M. Paschal. 1989. The role of dynein and other microtubule-activated ATPases in mitosis. *In* Mechanisms of Chromosome Distribution and Aneuploidy. M. A. Resnick, and B. K. Vig, editors. Alan R. Liss, Inc., New York. 205–215.
60. Walter, R. J., and M. W. Berns. 1987. Digital image processing and analysis. *In* Video Microscopy. S. Inoué, editor. Plenum Publishing Corp., New York. 327–392.
61. Weiss, D. G., F. Keller, J. Golden, and W. Maile. 1986. Towards a new classification of intracellular particle movement based on quantitative analysis. *Cell Motil. and Cytoskeleton.* 6:128–135.